A rigorous approach of determining FAO 56 dual crop coefficient using soil sensor measurements and inverse modeling techniques

Kefeng Zhang*, Howard W. Hilton, Duncan J. Greenwood, Andrew J. Thompson

Warwick-HRI, Warwick University, Wellesbourne, Warwick CV35 9EF, UK

*Corresponding author

Address: Warwick-HRI, Warwick University, Wellesbourne, Warwick CV35 9EF, UK

Tel: 0044 24 7657 4996

Fax: 0044 24 7657 4500

E-mail: kfzhang@hotmail.com

ABSTRACT

Accurate estimation of crop coefficients for evaporation and transpiration is of great importance in optimizing irrigation and modeling water and solute transfers in the soil-crop system. In this study we used inverse modeling techniques on soil sensor measurements at depths from the soil-crop system to estimate crop coefficients. An inverse model was rigorously formulated to infer the crop coefficients and the lengths of growth stages using the measured soil water potential at depths during crop growth. By applying a micro-genetic algorithm to the formulated inverse model, the optimum values of the crop coefficient and the corresponding length of growth stage were successfully deduced. It has been found that the lengths of both the initial and development growth stages of cabbage were 5 days shorter than those from the FAO56 (Irrigation and Drainage Paper by the FAO). The deduced crop coefficient for transpiration at the initial growth stage was 0.11; slightly smaller than 0.15 recommended by the FAO56, while at the mid-season growth stage, the deduced value of 0.95 was identical with the recommended value. Results show that the predictions of soil water potential using the obtained values of crop coefficients agreed well with the measurements throughout the entire growing period, indicating that the deduced crop coefficients were credible and appropriate for cabbage grown under the specific conditions of location and climate. It follows that the strategy presented in the study can enable accurate estimates of crop coefficients to be obtained from soil sensor measurements and inverse modeling techniques.

Key words: water dynamics, soil-crop system, agricultural water management, irrigation, inverse analysis.

1. Introduction

The Food and Agriculture Organization (FAO) of the United Nations in its Irrigation and Drainage Paper, FAO56, provides a means of estimating water requirement for various crops grown under different climate conditions (Allen et al., 1998), which has been widely accepted and applied across the world. However, the crop coefficients proposed by the FAO56 might not be universally accurate so there is a need for local calibration according to crop species, soil and climate conditions (Allen et al., 1998).

Numerous studies have been conducted, aimed at obtaining more appropriate crop coefficients under local conditions. Calibration of crop coefficients has been made with weighing lysimeter devices (Liu et al., 2002; Kang et al., 2003; Karam et al., 2006; López-Urrea et al., 2009; Liu and Luo, 2010). Techniques using data from soil sensors at various depths for estimating evapotranspiration have also been attempted (Mastrorilli et al., 1998; Nachabe et al., 2005; Fernández-Gálvez and Barahona, 2007). Recently, the eddy covariance techniques, a prime atmospheric flux measurement technique to measure and calculate vertical turbulent fluxes within atmospheric boundary layers, have also been tested in agriculture for measuring crop evapotranspiration (Kjaersgaard et al., 2008; Li et al., 2008; Sun et al., 2008). Other techniques of measuring actual evapotranspiration can be seen in the review by Rana and Katerji (2000). Whilst most of these techniques give promising estimates of actual evapotranspiration at a field scale, a common problem

is that these techniques alone are not capable of separating soil evaporation from crop transpiration. Further, the weighing lysimeter technique is labor intensive and expensive.

Numerical modeling techniques for water dynamics in the soil-crop system, on the other hand, have progressed greatly in the last couple of decades through advances of sciences in soil and plant and computing power. Many developed mechanistic models are now able to make reliable predictions of water movement in various processes in the soil-crop system, given accurate inputs (Šimůnek et al., 1992, 2005; Bastiaanssen et al., 2007; Kroes et al., 2008; Yang et al., 2009). In recent years, with the help of such mechanistic models, efforts have been made to use inverse modeling techniques to infer the soil hydraulic properties using the soil water content/potential measurement at depths down the profile from cropped or fallow soil, and research on this topic has been fruitful (Ines and Droogers, 2002; Jhorar et al., 2002; Ritter et al., 2003; Sonnleitner et al., 2003; Gómez et al., 2009; Zhang et al., 2010). These techniques, though promising, have not been applied to estimate FAO56 crop coefficients.

The principal aim of this study was to devise a strategy of using soil sensor measurements and inverse modeling techniques to provide an easy and accurate alternative to calibrate crop coefficients locally. In order to examine the reliability of the deduced crop coefficients, comparisons were carried out between the simulated results with the deduced crop coefficient values and the soil sensor measurements within their working range and those modeled using the values recommended by the FAO56. Since soil sensors are available nowadays which are inexpensive, simple to maintain and install, and accurate, the study provides a promising means of calibrating crop coefficients locally with ease and accuracy.

2. Materials and methods

2.1. Experiments

An experiment was carried out at Wellesbourne, UK (latitude: 52°12' N, longitude: 1°37' W) using a Dutch white cabbage (*cv. Eminence*, Tozer seeds, UK). The soil was classified as a sandy loam of the Wick series (Whitfield, 1974). Prior to planting, soil samples were taken at 10 cm intervals down to a depth of 1.2 m for measurements of physical properties. Soils were found to be generally uniform in both the topsoil of 30 cm and the subsoil, however, a slightly higher percentage of sand and a lower percentage of clay were contained in the subsoil than the topsoil (Table 1). The slightly higher bulk density in the subsoil was likely to have been due to soil compaction. The soil below 1.2 m depth was assumed to be identical to the soil immediately above.

The experimental design was a fully randomised block, with five replicates. The crop was transplanted on 29 April 2009 and harvested on 8 September 2009. The plots were 5.0 x 2.0 m. Plants were spaced 0.50 m between, and within rows. 300 kg N ha^{-1} and 100 kg K ha^{-1} were applied as NH_4NO_3 and K_2SO_4 respectively, a day before planting and was incorporated into the soil during cultivation. Immediately after planting, the crop was given approximately 10 mm irrigation by overhead oscillating line, after which drip irrigation, supplied by pressure compensated drippers (Netafim, Tel Aviv, Israel), was applied. Pests, diseases and weeds were effectively controlled throughout growth.

Three irrigation treatments were imposed on the experiment after crop establishment. One treatment followed growers practice, i.e. 20 mm irrigation for 25 mm loss of soil water, in applying water, but no efforts were made to measure soil water potential. The second treatment adopted the irrigation regime according to the FAO56 throughout growth. The soil water content in the root zone was maintained above the critical threshold value of $0.55\theta_{fc}+0.45\theta_{pwp}$ with θ_{fc} and θ_{pwp} being soil water content at field capacity and the permanent wilting point, respectively. The third treatment had a threshold value of soil water content which was 25% lower than that used in the second treatment. The dates and volumes of irrigation for each treatment are given in Table 2.

Soil water potential was measured at various depths in the second and third treatments using Watermark 200SS-v soil moisture sensors (Irrometer Company, USA). Such sensors are a granular matrix sensor that measures soil water potential indirectly using electrical resistance (Shock, 2004). They have widely been used on commercial farms for irrigation scheduling and for research applications. The sensor is inexpensive, simple to install and easy to maintain (Thompson et al., 2006). Furthermore, Watermark 200SS sensors have a relatively wide working range of -10 to -200 kPa (Armstrong, 1987; Spaans and Baker, 1992), and are able to provide an accurate measurement of soil water potential (Thompson et al., 2006). The sensors were installed in the soil on 10 June at depths of 10, 30, 50, 70, 90 and 100 cm. Each set of 6 sensors were installed at the centre of a set of four plants, 35 cm from the drip-emitter to the plants in each replicate plot. Sensors were wired to a datalogger (DL2e, Delta-T devices, Cambrige, UK), readings were taken hourly and the replicate sensor measurements at each depth were averaged.

Soil samples were taken on 1 May 2009 to determine soil moisture in the layers of 0-30 cm, 30-60 cm and 60-90 cm (Table 3). Meteorological data were recorded using an on-site station, situated approximately 100 m from the experimental site. The measured weather variables included maximum, mean and minimum air temperatures, total solar radiation, relative humidity, wind speed and precipitation. Air temperature and relative humidity were measured at 1.25 m above ground. All the measurements were taken at daily intervals and some of them are given in Fig. 1.

At harvest, ten guarded heads per plot were cut level with the soil. These heads were weighed for fresh weight yield. A representative sub-sample of this material was taken and weighed, then dried and reweighed for an estimation of dry matter percentage. Pits were dug at the end of the second and third treatments plots, so that a confirmation of rooting depth could be made. This was achieved by carefully excavating the soil and recording the maximum depth at which roots were found. There were no significant effects of irrigation treatment on total yield, expressed either on a fresh or dry weight basis. The data from the second treatment, i.e. irrigation according to the FAO56 guidance, is used in this study. The measured dry weight yields and rooting depth are given in Table 3.

2.2. Inverse modeling

Inverse modeling, unlike forward modeling, estimates optimum values of model parameters from measured data, instead of predicting state variables of the system from input.

2.2.1 Formulation of the inverse model and optimization algorithm

The principles behind the inverse modeling techniques involved three different steps: determining the number of parameters to be deduced, formulating the optimized function, and implementing an optimized algorithm. In the study, the parameters that were required included the durations of crop initial, developmental, mid-season and late season growth stages, L_{ini}, L_{dev}, L_{mid} and L_{late}, and their associated basal crop coefficients for transpiration K_{cb_ini}, K_{cb_mid} and K_{cb_end} as defined by the FAO56 and illustrated in Fig. 2. Since the total growth length is known, the vector of the parameters to be deduced for the inverse model is $\mathbf{x} = [L_{ini}, L_{dev}, L_{mid}, K_{cb\_ini}, K_{cb\_mid}, K_{cb\_end}]^{\mathrm{T}}$. The optimized function is the mean relative error square between simulated values and measurements of a given state variable. Thus the inverse model can mathematically be stated as:

To find: $\mathbf{x}$

Maximize: $$f(\mathbf{x}) = -\frac{1}{N}\sum_{i=1}^{N}\left[\frac{h_{mea}(t_i, z) - h(t_i, z, \mathbf{x})}{h_{mea}(t_i, z)}\right]^2 \quad (1)$$

Subject to: $$\underline{x_j} \le x_j \le \overline{x_j} \qquad (j = 1, 2, \ldots, 6) \quad (2)$$

$$\underline{h_{mea}} \le h_{mea} \le \overline{h_{mea}} \quad (3)$$

where f is the optimized function, $\mathbf{x}$ is the parameter vector, z (cm) is the vertical coordinate, h_{mea} (cm) and h (cm) are the measured and simulated soil water pressure head at depth z in the profile, respectively, t_i is the time when the i^{th} measurement is taken, N is

the number of measurements, $\underline{x_j}$ and $\overline{x_j}$ are the lower and upper boundaries of the parameter x_j, respectively, and $\underline{h_{mea}}$ and $\overline{h_{mea}}$ are the lower and upper threshold values within which the measured soil water potential is reliable.

The optimized function, Eq. (1), gives the identical weight to the measured values of soil water potential at various depths since there was only one type of measurement with the same accuracy. However, it should be pointed out that different weights in the optimized function should be considered if the measurements are not equally accurate to reflect the precision of the measurements, as suggested by Hollenbeck and Jensen (1998) and Hollenbeck et al. (2002).

In inverse modeling the reliability of the deduced parameters is dependent on other parameters required to run the forward model. Any serious bias in the values of the unfitted parameters will, of course, greatly affect the reliability of the fitted parameters. In the soil-crop system, the determination of soil hydraulic properties is often problematic. In this study, soil hydraulic properties were determined using the pedo-transfer functions (PTFs) approach proposed by Wösten et al. (1999), based on a study of more than 5000 soil samples across Europe. Since the proposed PTFs were aimed particularly at the European soils, the determination of the soil hydraulic properties in this study was reasonable. It is realized though that soil hydraulic properties deduced using the field evaporation experiments as demonstrated in Zhang et al. (2010) are more representative at a field scale. However, the measured data from the fallow soil was not available for this study.

The selection of an effective optimization algorithm is crucially important for solving the inverse model. Although there are many traditional algorithms available (Rao,

1984; Hopmans and Šimunek, 1999) and some successful studies of using the traditional algorithms in parameter identification (Zhang et al., 2008), a common problem is that these methods are only able to find a localized optimum solution, and the solution is highly dependent on the initial estimates of the deduced parameters. However, modern evolutionary algorithms such as genetic algorithms (GAs) overcome this problem (Goldberg, 1989). When GAs are applied, the optimized function Eq. (1) is termed as the fitness function. The software used in the study is for a micro-GA developed by Carroll (1999). It has been proved that the micro-GA technique is very effective, and was previously used for inferring soil hydraulic properties from the field evaporation experiments (Zhang et al., 2010).

2.2.2. Description of the forward flow model

To simulate the soil water pressure head at depths in the profile and at the time intervals required by Eq. (1), a forward model needs to run. The model outlined in this section is for this purpose, i.e. predicting spatial-temporal soil water pressure head during the simulation period. The justification of using the equations below is given in Yang et al. (2009) and Zhang et al. (2010). It has been demonstrated that if the environmental conditions, soil hydraulic properties and crop parameters are known with more precision, then the model is able to produce accurate results in predicting water dynamics in the soil-crop system (Yang et al., 2009).

In 1-D systems, the Richards' equation for water transfer within the soil profile, expressed in terms of soil water content, θ, and soil water pressure head, h, is:

$$\frac{\partial \theta}{\partial t} = \frac{\partial}{\partial z}[K(\theta)(\frac{\partial h}{\partial z} + 1)] - \beta(h) S_{\max}(z) \quad (4)$$

where K (cm d^{-1}) is the soil hydraulic conductivity, β is the root water stress reduction factor, and S_{max} (d^{-1}) is the maximum root water uptake.

The soil hydraulic functions are defined according to van Genuchten (1980) and Mualem (1976):

$$\Theta = \frac{\theta - \theta_r}{\theta_s - \theta_r} = [\frac{1}{1 + |\alpha h|^n}]^m \quad (5)$$

$$K(\theta) = K_s \Theta^{0.5}[1 - (1 - \Theta^{1/m})^m]^2 \quad (6)$$

where Θ is the relative saturation, θ_s and θ_r (cm^3 cm^{-3}) are the saturated and residual soil water contents, α (cm^{-1}) and n are the shape parameters of the retention and conductivity functions, m = 1-1/n, and K_s (cm d^{-1}) is the saturated hydraulic conductivity.

S_{max} and β can be calculated using the following expressions (Feddes et al., 1978; Wu et al., 1999; Yang et al., 2009; Zhang, 2010; Zhang et al., 2010):

$$S_{\max}(z) = L_r(z) K_{cb} ET_0 / \Sigma L_r(z) \quad (7)$$

$$\beta(h) = \begin{cases} 0 & h \le h_3 \text{ , } h \ge h_1 \\ (h - h_3)/(h_2 - h_3) & h_3 < h < h_2 \\ 1 & h_2 \le h < h_1 \end{cases} \quad (8)$$

where $L_r(z)$ is the relative root length distribution at z, K_{cb}, is the basal crop coefficient for transpiration from the FAO56, dependent on crop species and its development stage, ET_0 (mm) is the reference evapotranspiration, h_3 is the soil water pressure head at the permanent wilting point (-15,000 cm), h_1 is the soil water pressure head near saturation above which water uptake is prohibited due to the lack of oxygen (-1 cm), and h_2 is the threshold soil water pressure head below which the transpiration is reduced. For a rapid transpiration of 5 mm d^{-1} and a slow transpiration of 1 mm d^{-1}, h_2 has values of -500 cm and -1,100 cm, respectively (Šimůnek et al., 1992; Sonnleitner et al., 2003; Yang et al., 2009).

ET_0 can be estimated using a Penman-Monteith method directly at daily intervals according to the FAO56:

$$ET_0 = \frac{0.408\Delta(R_n - G) + 900\gamma/(T+273)u_2(e_s - e_a)}{\Delta + \gamma(1 + 0.34u_2)} \quad (9)$$

where R_n (MJ m^{-2} d^{-1}) is the net radiation at the crop surface, G (MJ m^{-2} d^{-1}) is the soil heat flux density, u_2 (m s^{-1}) is the 24 h average wind speed at 2 m height, e_s (kPa) is the saturation vapour pressure, e_a (kPa) is the actual vapor pressure, Δ (kPa °C^{-1}) is the slope of the vapour pressure curve, and γ (kPa °C^{-1}) is the psychrometric constant. The procedures of computing G, e_s, e_a, δ and γ are given in the FAO56.

The net radiation at the crop surface is calculated as suggested by the FAO56:

$$R_n = 0.77 R_s - 2.45 \times 10^{-9}[(T_{\max} + 273.3)^4 + (T_{\min} + 273.3)^4](0.34 - 0.14 e_a^{0.5})[\frac{1.35 R_s}{(0.75 + 0.00002\ z_{alt}) R_a} - 0.35] \quad (10)$$

in which

$$e_a = 0.003054(e^{\frac{17.27 T_{\min}}{T_{\min} + 237.3} RH_{\max}} + e^{\frac{17.27 T_{\max}}{T_{\max} + 273.3} RH_{\min}}) \quad (11)$$

$$R_a = \frac{24 \times 60}{\pi} \times 0.082 d_r [\omega_s \sin(\varphi)\sin(\delta) + \cos(\varphi)\cos(\delta)\sin(\omega_s)] \quad (12)$$

$$d_r = 1 + 0.033 \cos(\frac{2\pi}{365} J) \quad (13)$$

$$\delta = 0.409 \sin(\frac{2\pi}{365} J - 1.39) \quad (14)$$

$$\omega_s = \arccos[-\tan(\varphi)\tan(\delta)] \quad (15)$$

where R_s (MJ $m^{-2}d^{-1}$) is the daily total solar radiation, T_{min} and T_{max} (°C) are the daily minimum and maximum air temperature, respectively, z_{alt} (m) is the altitude, RH_{min} and RH_{max} (%) are the daily minimum and maximum relative humidity, respectively, d_r is the relative distance between the earth and the sun, J is the day number in the year, δ (radian) is the solar declination, φ (radian) is the latitude, and ω_s is the sunset hour angle.

Rooting depth growth is estimated according to Greenwood et al. (1982) and Zhang et al. (2007; 2009):

$$R_z = R_{z0} + \max[0, 10(W - 2)] \quad (16)$$

where R_z (cm) is the rooting depth, R_{z0} is the rooting depth at planting (assumed 20 cm for a vegetable crop with dry weight less than 2 t ha^{-1}), W (t ha^{-1}) is the above ground plant dry weight, which is estimated by the following equation for daily increments (Greenwood et al., 1977; Zhang et al., 2007, 2009):

$$\Delta W = \frac{W}{1+W} \frac{\ln(W_{\max} / W_0) + W_{\max} - W_0}{T_{growth}} \quad (17)$$

in which W_0 and W_{max} are the crop dry weights at planting and harvest. T_{growth} (d) is the length of the total growth period.

The root length density declines exponentially from the soil surface downwards (Gerwitz and Page, 1974; Pedersen et al., 2010):

$$L_r(z) = e^{-a_z z} \qquad z \le R_z \quad (18)$$

where a_z (cm^{-1}) is the shape parameter controlling root distribution down the soil profile.

Daily potential soil evaporation is calculated using the dual crop coefficient method proposed by the FAO56:

$$E_{pot} = K_e ET_0 \quad (19)$$

where E_{pot} (cm) is the potential daily soil evaporation, ET_0 (cm) is the reference evapotranspiation, and K_e is the evaporation coefficient, defined as:

$$K_e = \min[K_{c\max} - K_{cb}, (1 - f_{cover})K_{c\max}] \quad (20)$$

where K_{cmax} is the maximum evapotranspiration coefficient, and f_{cover} is the soil fraction covered by plants, calculated according to the assumption that the proportion of crop ground cover is linearly related to W and the full cover occurs when W reaches 4 t ha^{-1} for cabbage crop measured from the previous experiments (unpublished data).

The dual crop coefficients used in this study, i.e. K_{cb} in Eq. (7) and K_e in Eq. (19), are to calculate potential soil evaporation and crop transpiration at a given day. The calculated potential soil evaporation is applied to the soil surface for computing actual evaporation, whereas the potential crop transpiration is applied in the root zone as expressed in Eq. (7) for computing actual root water uptake in the forward flow model. Whether the potential soil evaporation and crop transpiration are met is dependent on the water availability in the soil.

The procedure used to solve the forward flow model formulated above was that proposed by Yang et al., (2009). The proposed approach, based on the work by Lee and Abriola (1999), considers that water content in a soil layer is only influenced by the layers above and below in a small time step of 0.001 d, which drastically simplifies the algorithm, allowing soil water flow to be calculated layer by layer. The procedure works with a uniform 5 cm soil layer, and the soil layer is numbered 1 at the bottom of the profile and with the layer number increasing towards the surface. For re-distribution of soil water in the profile, the integrated form of Eq. (4) is applied from the bottom layer to

the top layer at each time step. A detailed description of the algorithm is given elsewhere (Yang et al., 2009).

2.2.3. Implementation procedure

To identify the parameter vector **x** which contains the crop coefficients and the durations of crop initial, development, mid-season and the late growth stages, the following procedures have to be implemented:

1) Set the lower and upper boundaries of the parameter vector **x,** numbers of population and generation for the micro-GA algorithm;
2) Randomly generate a population of abstract representations of candidate solutions;
3) Calculate daily soil water potential values at depths where sensors are placed using the forward flow model for a given candidate solution in the population;
4) Calculate the fitness function f (Eq. 1) using the calculated and measured soil water potential values;
5) Repeat 3) and 4) for all the candidate solutions in the population;
6) Evaluate every candidate solution in the population based on their fitness (the higher the f value, the better);
7) Form a new population through genetic operators of crossover and mutation;
8) Repeat from 3) to 7) until the maximum number of generations produced;
9) Find the best solution in the population of the last generation.

The descriptions of the terminologies regarding GAs and how the genetic operators are performed can be seen in Goldberg (1989).

2.2.4. Evaluation criteria

Accuracy of the simulated soil water pressure head using deduced parameter values was evaluated as the Nash-Sutcliffe efficiency (NSE) (Nash and Sutcliffe, 1970) and the root of the mean squared errors (RMSE):

$$NSE = 1 - \frac{\sum_{i=1}^{N}[h_{mea}(t_i, z) - h(t_i, z)]^2}{\sum_{i=1}^{N}[h_{mea}(t_i, z) - h_{mea}^{'}]^2} \quad (21)$$

$$RMSE = \sqrt{\frac{1}{N}\sum_{i=1}^{N}[h_{mea}(t_i, z) - h(t_i, z)]^2} \quad (22)$$

where $h_{mea}^{'}$ is the average of the measured values.

A value of NSE close to 1 and a small RMSE indicate that the simulated values are in good agreement with the measured values.

2.2.5 Parameter values

The information required for the inverse model includes the upper and lower boundaries of the deduced variables, weather data, soil hydraulic properties, together with the crop parameters and the initial conditions for running the forward flow model. The lower and upper boundaries set for the parameter vector of crop coefficient and length of

growth stage were $\underline{\mathbf{x}} = [L_{ini}, L_{dev}, L_{mid}, K_{cb\_ini}, K_{cb\_mid}, K_{cb\_end}]^T = [25, 65, 100, 0.1, 0.7, 0.7]^T$ and $\bar{\mathbf{x}} = [L_{ini}, L_{dev}, L_{mid}, K_{cb\_ini}, K_{cb\_mid}, K_{cb\_end}]^T = [50, 90, 125, 0.3, 1.2, 1.2]^T$. $\underline{h_{mea}}$ and $\overline{h_{mea}}$ in Eq. (3) were -2000 cm and -100 cm soil water pressure head, respectively, corresponding to the soil water potential of -200 kPa and -10 kPa within which the soil sensors perform reliably (Thomson and Armstrong, 1987; Spaans and Baker, 1992). The weather data used in the simulation periods, including daily minimum and maximum air temperatures, rainfall, global radiation, relatively humidity and wind speed were measured and some of the measurements are given in Fig. 1. Since no measurement of solar radiation was made from 13 August to 20 August 2009, the measured pan evaporation was used in estimating reference evapotranspiration in the subsequent simulations for the period.

Soil water retention curves for the topsoil (0 - 30 cm) and the subsoil (30 cm -) were derived using the PTFs proposed by Wösten et al. (1999). The PTFs, derived based on a study of extensive EU soil samples, is considered particularly appropriate for the soils used in the study. Soil water was calculated to a depth of 200 cm. The calculated soil domain was down to 200 cm. The soil hydraulic properties derived using the PTFs for the topsoil and subsoil are listed in Table 1. The measured final dry weight yield (Table 3) was used in estimating rooting depth during growth (Eqs. 16, 17). The shape parameter controlling root distribution down the soil profile a_z in Eq. (18) was set to be 0.03 cm^{-1}, within the range measured for vegetable crops (Greenwood et al., 1982). We used the measured soil water distributions down the profile on 1 May 2009 as the initial conditions (Table 1). The soil water between the deepest measured depth and 200 cm was assumed to be at equilibrium.

3. Results and discussion

3.1 Crop coefficient and length of growth stage

The lengths of different crop growth stages and their associated crop coefficients for transpiration were successfully obtained by solving the inverse model formulated in Eq. (1) using the micro-GA technique. The deduced parameter vector for crop coefficient and length of growth stage was $\mathbf{x} = [L_{ini}, L_{dev}, L_{mid}, K_{cb\_ini}, K_{cb\_mid}, K_{cb\_end}]^T = [35, 55, 17, 0.11, 0.95, 0.89]^T$. It can be observed that while the obtained K_{cb_ini} of 0.11 at the initial growth stage is slightly smaller than 0.15 by the FAO56, the value of K_{cb_mid} at the mid-season growth stage is the same as the recommendation, i.e. 0.95 (Fig. 3). The lengths of the initial and development growth stages were 35 days and 55 days, respectively, 5 days less than the FAO56 recommendations on each occasion. However the mid-season growth stage was markedly shorter than the recommended value and the difference was 35 days. The length and crop coefficient value for the late growth stage obtained from the study were 25 days and 0.89, compared with 15 days and 0.85 by the FAO56. The difference between the deduced K_{cb_mid} and K_{cb_end} was 0.06, smaller than 0.1 as suggested by the FAO56. The differences in the parameter values between the deduced and recommended may be attributed to the crop cultivar and the climate under which the crop grew. Another contributory factor for the smaller difference in K_{cb} between the mid-season and late growth stages is that the total growing period in the experiment was considerably shorter than that assumed by the FAO56. The plants at harvest were not

mature enough to significantly reduce transpiration. Overall the deduced parameter values for crop coefficient and length of growth stage are credible (Fig. 3).

The deduced values are somewhat different from the FAO56 recommendations. Results reveal that the lengths of initial and development growth stages for cabbage grown in the experiment are slightly shorter than the FAO56 recommendation, and so is the crop coefficient for transpiration at the initial growth stage. Such a phenomenon that the deduced crop coefficients deviate from the FAO recommended values has been widely reported for a range of crops (Kang et al., 2003; López-Urrea et al., 2009). Length of crop growth stages may differ under different climates, and different cultivars may have different transpiration rates, root distributions as well as different lengths of growth stages (Tuberosa, 2004; Tardieu, 2005). It is therefore necessary to calibrate the crop coefficient locally so that the water application can be managed more precisely.

It should also be pointed out that, despite the big difference in irrigation amount applied according to the growers practice (110 mm) and the FAO56 guidance (56 mm), there was no significant difference in terms of crop dry weight yield. This suggests that the maximum crop growth can be obtained when the soil moisture content in the root zone is far below that at field capacity, and the threshold value of soil water content in the root zone for irrigation by the FAO56 is reasonable for cabbage in this study, in agreement with the previous studies using the same approach for irrigation for other crops (see the review by Greenwood et al., 2010). It follows that the FAO56 provides a good guidance for optimal irrigation over a wide range of crops, and potentially has benefits over existing grower practices.

3.2 Performance of the forward flow model

Fig. 4 shows the overall comparison of soil water potential between measurement and simulation for the measured range of -10 to -200 kPa within which the sensors work accurately. The simulated values were obtained using the forward flow model with the deduced crop parameter values. Regression between measurement and simulation gave a high value of R^2 (0.814) and approximately 1 (0.995) for the gradient (Fig. 4). Statistical analyses (Eqs. 21, 22) also gave a high value of NSE (0.78) and a relatively low value of RMSE (15.3 kPa). This indicates that the overall agreement between measurement and simulation is satisfactory. For comparison, the simulations were also carried out using the FAO56 recommended values and the same statistical analyses were applied to the simulated results. Likewise the statistical indices were 0.64 for NSE and 20.0 kPa for RMSE, respectively. The agreement between measurement and simulation is evidently worse than that obtained with the obtained crop parameter values. This partly reconfirms the reliability of the deduced parameters.

Detailed comparison of the soil water potential at various depths between measurement and simulation was also carried out (Fig. 5). The model not only reproduced the patterns of soil water changes in layers, but also produced values close to the measurements. At the 10cm and 30cm depths, soil water potential was markedly affected by rainfall. The peaks of soil water potential (most negative) all coincided with the end of the dry spell of weather. However, in the subsoil (below 30 cm) the soil water potential was much less affected by rainfall (Fig. 5). While the overall performance of the forward model in reproducing the measurements is fairly good, discrepancies also exist

between measurement and simulation. The simulated soil water potential at the 10 cm depth agree well with the measured values, but at the deeper depths the discrepancies between measurement and simulation tended to increase. One possible reason is the simple assumption about root length distribution. The model assumes that the root length distribution during growth is exponential down the profile from the surface and there is only one parameter controlling the distribution. Results from the study indicate that the assumption might be an over-simplification. In the model a_z is the only parameter controlling root length distribution down the profile. There is no flexibility to distribute roots other than the exponential manner, whereas the root distribution has not always found to be exponential in field experiments (Thorup-Kristensen, 2006). Consideration should be given to formulate the root distribution in a different way with more parameters such as polynomial distribution proposed by Wu et al. (1999) so that the modeling of root distribution can be carried out more accurately. Also, attempts should be made to infer the root parameters together with other crop parameters from the soil sensor measurements at depths. Another contributory factor is the dynamic impact of water stress on root water uptake. It has been found that water stress that occurs in one part of the root zone can be compensated for by enhanced extraction from the other wetter parts (Lai and Katul, 2000; Li et al., 2001; Yadav et al., 2009). When the top soil dries, the roots in the deep wetter soil increase their capacity of extracting water, which could lead to lower than the simulated water potential in the deep soil as shown in Fig. 5. To further improve the forward flow model, root water uptake with water stress compensation should be incorporated in the future.

3.3 Simulated crop coefficients and evapotranspiration

Daily simulated crop transpiration coefficient and soil evaporation coefficient according to Eq. (20) are shown in Fig. 6(a). Despite the fluctuation in K_{cb} which was caused by the environmental factor, the simulated K_{cb} does not deviate markedly from the basal lines. It follows that the potential transpiration was basically met, and the crop did not suffer water stress throughout growth. The evaporation coefficient K_e, on the other hand, varies greatly at the initial crop growth stage, followed by a steady decline before reaching zero on 30 June when full ground cover occurred. The large variations in K_e at the initial growth stage were due to the changes in soil water in the surface soil. The maximum soil evaporation occurred after an event of rainfall or irrigation when the top soil was wet. The simulated single crop coefficient K_c, i.e. the sum of the K_{cb} and K_e as defined by the FAO56, is also compared with the recommendations (Fig. 6b). While generally the simulated K_c follows the FAO lines, the simulated values are somewhat lower than the recommended values at the early development growth stage, possibly caused by obtained shorter lengths of the initial and development growth stages. At the initial crop growth stages, the calculated K_c fluctuates greatly, similar with the soil evaporation coefficient K_e.

Fig. 7 shows the cumulative potential and simulated evapotranspiration during growth, together with the cumulative rainfall plus irrigation. It reveals that the cumulative actual evapotranspiration was about 55 mm less than the cumulative potential evapotranspiration, which can be attributed to the dry spell between 22 May and 01 June when no irrigation was applied. Further, it can be observed that the crop

evapotranspiration was mainly met by the rainfall and irrigation. The cumulative simulated evapotranspiration at harvest was 351 mm, compared with 316 mm provided by rainfall and irrigation. Also, soil water initially contained in the profile contributed to the crop evapotranspiration as soil water potential in all layers was lower at harvest than at planting time.

3.4 Rooting depth and root length distribution

Fig. 8 shows the rooting depth estimated in the study using Eqs. (16) and (17) against the cumulative daily air temperature. It reveals that the rooting depth started to increase (when the above ground dry weight reached 2 t ha^{-1}) at the cumulative day degree of approximately 500 $d^{o}C$ after planting, and the increment in rooting depth is virtually related to the cumulative daily air temperature in a linear manner. The root growth rate was approximately 0.8 cm $d^{-1o}C^{-1}$. This indicates that after a threshold of cumulative day temperature from planting, the increase in rooting depth could also be linearly correlated with the cumulative day temperature, in agreement with the experimental evidence (Thorup-Kristensen, 1998, 2006; Thorup-Kristensen and Van den Boogaard, 1999; Kage et al., 2000). The threshold value of 500.0 $d^{-1o}C^{-1}$ and the growth rate of approximately 0.8 mm $d^{-1o}C^{-1}$ in the study are higher than 350 - 400 $d^{-1o}C^{-1}$ and lower than 1.2 mm $d^{-1o}C^{-1}$ reported by Thorup-Kristensen (2006) for cabbage. Given the fact that the predicted maximum rooting depth by Eq. (16) is in good agreement with the measured value of 140 cm, the threshold value of 500 $d^{-1o}C^{-1}$ and 0.8 mm $d^{-1o}C^{-1}$ growth rate were more appropriate for the crop grown on this particular site, suggesting that the

growth rate might not be universally held and should be calibrated locally. The differences in both the threshold value and the growth rate might be caused by different soils having different mechanical impedance to root elongation and the cultivars used in the experiments.

The effect of the shape parameter controlling root length distribution down the profile a_z on overall model prediction of soil water potential at different depths was investigated. The regressions between measurement and simulation without the intercept using various a_z values of 0.02, 0.025, 0.03, 0.035 and 0.04 cm^{-1} were performed at all depths (Fig. 9) and the regressed coefficients of the best fitted lines are listed Table 4. There is a trend that the gradient of the fitted lines decreases with increasing a_z (Table 4). A smaller value of a_z gives more uniformly distributed root length down the profile, while a bigger value produces more roots near the surface. It is evident that if a_z is unrealistically low or high the fitted line deviates from the 1:1 line greatly (Fig. 9). It can be concluded from Table 4 that a_z of 0.03 cm^{-1} is the most appropriate to use in Eq. (18) describing root length distribution in the profile for cabbage, as detailed in the study.

3.5 Application of the calibrated model

With the advances in mathematics and computer sciences, modeling has increasingly become an important tool in precision agriculture. Bastiaanssen et al. (2007) reported that the mechanistic models could and should be used in assisting irrigation scheduling. Greenwood et al. (2010) argued that sufficient advances have been made in soil and plant sciences as well as in sensor and wireless technologies, such to merit

applying the quantitative models to optimizing irrigation. Nevertheless, the models of this kind in practical use are still low (Bastiaanssen et al., 2007). Apart from the difficulty in estimating soil hydraulic properties (Bastiaanssen et al., 2007), we believe that the lack of confidence in the model predictions is another primary reason why people do not take the models seriously. Indeed, using the model without calibration for studying water dynamics in the soil-crop system and irrigation scheduling is not always reliable since the system is extremely complex. As sensor-driven irrigation systems become more affordable and more widely adopted, efforts should be made to feed the models with the measurements for calibration to improve the accuracy of model predictions. It is easy nowadays to develop and calibrate the models to produce reasonable predictions in a given location for a number of crops. Together with the knowledge of the tolerance of water stress in terms of either soil water content in the FAO56 or soil water potential (Kroes et al., 2008) for various crops, this could lead to irrigation scheduling which solely relies on the calibrated models. Furthermore, due to the indispensable relationship between soil water and the availability of nutrients for uptake by roots, the models calibrated in this way undoubtedly improve the model-based decision support systems for fertilizer requirement in crop production such as those developed by Zhang et al. (2007, 2009) and Zhang (2010).

4. Conclusions

A strategy of inferring the lengths of different crop growth stages and the crop coefficient by applying an inverse modeling approach on the soil water potential data

collected from depths has been devised. The soil water potential values obtained from the model using the deduced parameter values were in much better agreement with the measured values than if the FAO56 recommended parameter values were used. This suggests that the strategy presented in the study should enable more accurate estimates of crop water requirements to be made. We are moving to a situation where accurate sensor measurements of water potential or content can be obtained at different depths down the soil profile with a reasonable cost. If this objective is met then the procedures proposed in this paper provide an easy, affordable and accurate alternative of calibrating crop coefficients locally for precise and efficient water management in crop production.

It was also found that the micro-GA algorithm was a powerful and robust tool to find the global solution to the optimization problem. The predicted rooting depth increased with cumulative day temperature linearly. It is necessary to estimate the root growth rate using the measured/estimated maximum rooting depth and cumulative day temperature during growth when applying the inverse modeling technique. Further work is required to improve the forward flow model by incorporating water stress compensation for root water uptake, and to expand the inverse modeling technique so that all the crop parameters including those describing root growth dynamics can be obtained. These improved model predictions will allow irrigation scheduling to be finely tuned to the requirements of local conditions.

Acknowledgements

The authors are grateful to the financial support to carry out the work as part of the WaterBee project (Grant Agreement Number: 222440) funded by the Seventh Framework Programme of the European Community for research, technological development and demonstration activities (2007-2013) under the Specific Programme "Capacities" (Research for the Benefit of SMEs).

References

Allen, R.G., Pereira, L.S., Raes, D., Smith, M., 1998. Crop evapotranspiration. Guidelines for computing crop water requirements. FAO Irrigation and Drainage Paper 56. FAO, Rome.

Bastiaanssen, W.G.M., Allen, R.G., Droogers, P., D'Urso, G., Steduto, P., 2007. Twenty-five years modeling irrigated and drained soils: State of the art. Agric. Water Manage. 34, 137–148.

Carroll, D.L., 1999. http://cuaerospace.com/carroll/ga.html.

Feddes, R.A., Kowalik, P.J., Zaradny, H., 1978. Water uptake by plant roots. In: Feddes, R.A., Kowalik, P.J., Zaradny, H. (Eds.), Simulation of Field Water Use and Crop Yield. John Wiley & Sons, Inc., New York, pp. 16-30.

Fernández-Gálvez, J., Verhoef, A., Barahona, E., 2007. Estimating soil water fluxes from soil water records obtained using dielectric sensors. Hydrol. Process. 21, 2785-2793.

Gerwitz, A., Page, E.R., 1974. Empirical mathematical model to describe plant root systems 1. J. Appl. Ecol. 11, 773-781.

Goldberg, D.E., 1989. Genetic Algorithms in Search, Optimization and Machine Learning. Addison-Wesley, Reading, Mass.

Gómez, S., Severino, G., Randazzo, L., Toraldo, G., Otero, J.M., 2009. Identification of the hydraulic conductivity using a global optimization method. Agric. Water Manage. 96, 504-510.

Greenwood, D.J., Cleaver, T.J., Loquens, S.H.M., Niendorf, K.B., 1977. Relationships between plant weight and growing period for vegetable crops in the UK. Ann. Bot. 41, 987-997.

Greenwood, D.J., Gerwitz, A., Stone, D.A., Barnes, A., 1982. Root development of vegetable crops in the UK. Plant Soil 68, 75-92.

Greenwood, D.J., Zhang, K., Hilton, H.W., Thompson, A.J., 2010. Opportunities for improving of irrigation efficiency with quantitative models, soil water sensors and wireless technology. J. Agric. Sci. 148, 1-16.

Hollenbeck, K.J, Jensen, K.H., 1998. Maximum-likelihood estimation of unsaturated hydraulic parameters. J. Hydrol. 210, 192-205.

Hollenbeck, K.J., Šimunek, J., van Genuchten, M.Th., 2000. RETMCL: Incorporating maximum-likelihood estimation principles in the RETC soil hydraulic parameter estimation code. Comput. Geosci. 26, 319-327.

Hopmans, J.H., Šimunek, J., 1999. Review of inverse estimation of soil hydraulic properties. In: Van Genuchten, M.Th., Leij, F.J., Wu, L. (Eds.), Characterization and Measurement of the Hydraulic Properties of Unsaturated Porous Media. University of California, CA, pp. 634-659.

Ines, A.V.M., Droogers, P., 2002. Inverse modeling in estimating soil hydraulic functions: a Genetic Algorithm approach. Hydrol. Earth Syst. Sci. 6, 49-65.

Jhorar, R.K., Bastiaanssen, W.G.M., Feddes, R.A., Van Dam, J.C., 2002. Inversely estimating soil hydraulic functions using evapotranspiration fluxes. J. Hydrol. 258, 198-213.

Kage, H., Kochler, M., Stutzel, H., 2000. Root growth of cauliflower (*Brassica oleracea* L. botrytis) under unstressed conditions: measurement and modelling. Plant Soil 223, 131-145.

Kang, S., Gu, B., Du, T., Zhang, J., 2003. Crop coefficient and ratio of transpiration to evapotranspiration of winter wheat and maize in a semi-humid region. Agric. Water Manage. 59, 239-254.

Karam, F., Lahoud, R., Masaad, R., Daccache, A., Mounzer, O., Rouphael, Y., 2006. Water use and lint yield response of drip irrigated cotton to the length of irrigation season. Agric. Water Manage. 16, 287-295.

Kjaersgaard, J.H., Plauborg, F., Mollerup, M., Petersen, C.T., Hansen, S., 2008. Crop coefficients for winter wheat in a sub-humid climate regime. Agric. Water Manage. 95, 918-924.

Kroes, J.G., Van Dam, J.C., Groenendijk, P., Hendriks, R.F.A., Jacobs, C.M.J., 2008. SWAP version 3.2. Theory Description and User Manual. Wageningen, Alterra, Alterra Report1649, 262 pp.

Lai, C.T., Katul, G., 2000. The dynamic role of root-water uptake in coupling potential to actual transpiration. Adv. Water Resour. 23, 427–439.

Lee, D.H., Abriola, L.M., 1999. Use of the Richards equation in land surface parameterizations. J. Geophys. Res. 104, 27519-27526.

Li, K.Y., De Jong, R., Boisvert, J.B., 2001. An exponential root water-uptake model with water stress compensation. J. Hydrol. 252, 189–204.

Li, S., Kang, S., Li, F., Zhang, L., 2008. Evapotranspiration and crop coefficient of spring maize with plastic mulch using eddy covariance in northwest China. Agric. Water Manage. 95, 1214-1222.

Liu, C., Zhang, X., Zhang, Y., 2002. Determination of daily evaporation and evapotranspiration of winter wheat and maize by large-scale weighing lysimeter and micro-lysimeter. Agric. Forest Meteorol. 111, 109-120.

Liu, Y., Luo, Y., 2010. A consolidated evaluation of the FAO-56 dual crop coefficient approach using the lysimeter data in the North China Plain. Agric. Water Manage. 97, 31-40.

López-Urrea, R., Martín de Santa Olalla, F., Montoro, A., López-Fuster, P., 2009. Single and dual crop coefficients and water requirements for onion (*Allium cepa* L.) under semiarid conditions. Agric. Water Manage. 96, 1031-1036.

Mastrorilli, M., Katerji, N., Rana, G., Nouna, B.B., 1998. Daily actual evapotranspiration measured with TDR technique in Mediterranean conditions. Agric. Forest Meteorol. 90, 81-89.

Mualem, Y., 1976. A new model for predicting the hydraulic conductivity of unsaturated porous media. Water Resour. Res. 12, 513-522.

Nachabe, M., Shah, N., Ross, M., Vomacka, J., 2005. Evapotranspiration of two vegetation covers in a shallow water table environment. Soil Sci. Soc. Am. J. 69, 492-499.

Nash, J.E., Sutcliffe J.V., 1970. River flow forecasting through conceptual models part I - A discussion of principles. J. Hydrol. 10, 282–290.

Pedersen, A., Zhang, K., Thorup-Kristensen, K., Jensen, L.S., 2010. Modelling diverse root density dynamics and deep nitrogen uptake – A simple approach. Plant Soil 326, 493-510.

Rana, G., Katerji, N., 2000. Measurement and estimation of actual evapotranspiration in the field under Mediterranean climate: a review. Eur. J. Agron. 13, 125-153.

Rao, S.S., 1984. Optimization: Theory and Application. Wiley Eastern Limited.

Ritter, A., Hupet, F., Munoz-Carpena, R., Lambot, S., Vanclooster, M., 2003. Using inverse methods for estimating soil hydraulic properties from field data as an alternative to direct methods. Agric. Water Manage. 59, 77-96.

Romano, N., Santini, A., 1999. Determining of soil hydraulic functions from evaporation experiments by a parameter estimation approach: experimental verifications and numerical studies. Water Resour. Res. 35, 3343-3359.

Šimůnek, J., Vogel, T., Van Genuchten, M.Th., 1992. The SWMS_2D code for simulating water flow and solute transport in two-dimensional variably saturated media, v 1.1, Research Report No. 126, U. S. Salinity Lab, ARS USDA, Riverside, CA.

Šimůnek, J., van Genuchten, M.Th., Šejna, M., 2005. The HYDRUS-1D software package for simulating the one-dimensional movement of water, heat, and multiple

solutes in variably-saturated media. Version 3.0. HYDRUS Softw. Ser. 1. Department of Environmental Sciences, University of California, Riverside, CA.

Shock, C.C., 2004. Granular matrix sensors, http://www.cropinfo.net/granular.htm.

Sonnleitner, M.A., Abbaspour, K.C., Schulin, R., 2003. Hydraulic and transport properties of the plant–soil systems estimated by inverse modelling. Eur. J. Soil Sci. 54, 127-138.

Spaans, E.J.A., Baker, J.M., 1992. Calibration of Watermark soil moisture sensors for soil matric potential and temperature. Plant Soil 143, 213-217.

Sun, G., Noormets, A., Chen, J., McNulty, S.G., 2008. Evapotranspiration estimates from eddy covariance towers and hydrologic modeling in managed forests in Northern Wisconsin, USA. Agric. Forest Meteorol. 148, 257-267.

Tardieu, F. 2005. Plant tolerance to water deficit: physical limits and possibilities for progress. C. R. Geosci. 337, 57–67.

Thomson, S.J., Armstrong, C.F., 1987. Calibration of the Watermark 200 model soil moisture sensor. Appl. Eng. Agric. 12, 99-103.

Thorup-Kristensen, K., 1998. Root growth of green pea (*Pisum sativum* L.) genotypes. Crop Sci. 38, 1445-1451.

Thorup-Kristensen, K., 2006. Root growth and nitrogen uptake of carrot, early cabbage, onion and lettuce following a range of green manures. Soil Use Manage. 22, 29-38.

Thorup-Kristensen, K., Van den Boogaard, R., 1999. Vertical and horizontal development of the root system of carrots following green manure. Plant Soil 212, 145-153.

Tuberosa, R. 2004, Molecular approaches to unravel the genetic basis of water use efficiency. In: Bacon, M.A. (Ed.), Water Use Efficiency in Plant Biology. Blackwell, Oxford, pp. 228-301.

Van Genuchten, M.Th., 1980. A closed-form equation for predicting the hydraulic conductivity of unsaturated soils. Soil Sci. Soc. Am. J. 44, 892-898.

Whitfield, W.A.D., 1974. The soils of the National Vegetable Research Station, Wellesbourne. pp.21-30. In: Report of the National Vegetable Research Station for 1973. The British Society for the promotion of vegetable research Wellesbourne UK.

Wösten, J.H.M., Lilly, A., Nemes, A., Le Bas, C., 1999. Development and use of a database of hydraulic properties of European soils. Geoderma 90, 169-185.

Wu, J., Zhang, R., Gui, S., 1999. Modeling soil water movement with water uptake by roots. Plant Soil 215, 7-17.

Yadav, B.K., Mathur, S., Siebel, M.A., 2009. Soil moisture dynamics modeling considering the root compensation mechanism for water uptake by plants. J. Hydrol. Eng. 14, 913-922.

Yang, D., Zhang, T., Zhang, K., Greenwood, D.J., Hammond, J., White, P.J., 2009. An easily implemented agro-hydrological procedure with dynamic root simulation for water transfer in the crop-soil system: validation and application. J. Hydrol. 370, 177-190.

Zhang, K., 2010. Evaluation of a generic agro-hydrological model for water and nitrogen dynamics (SMCR_N) in the soil-wheat system. Agric. Ecosyst. Environ. 137, 202-212.

Zhang, K., Greenwood, D.J., White, P.J., Burns, I.G., 2007. A dynamic model for the combined effects of N, P and K fertilizers on yield and mineral composition; description and experimental test. Plant Soil 298, 81-98.

Zhang, K., Burns, I.G., Turner, M.K., 2008. Derivation of a dynamic model of the kinetics of nitrogen uptake throughout the growth of lettuce: calibration and validation. J. Plant Nutr. 31, 1440-1460.

Zhang, K., Yang, D., Greenwood, D.J., Rahn, C.R., Thorup-Kristensen, K., 2009. Development and critical evaluation of a generic 2-D agro-hydrological model (SMCR_N) for the responses of crop yield and nitrogen composition to nitrogen fertilizer. Agric. Ecosyst. Environ. 132, 160-172.

Zhang, K., Burns, I.G., Greenwood, D.J., Hammond, J.P., White, P.J., 2010. Developing a reliable strategy to infer the effective soil hydraulic properties from field evaporation experiments for agro-hydrological models. Agric. Water Manage. 97, 399-409.

Figure captions

Fig. 1. Measured daily mean air temperature and relative humidity (a) and solar radiation and rainfall (b) during the experiment.

Fig. 2. Schematic diagram of the lengths of crop growth stages and crop coefficient for transpiration.

Fig. 3. Comparison of the lengths of various crop growth stages and crop coefficient for transpiration between inferred in the study and FAO56 recommendations.

Fig. 4. Overall comparison of soil water potential at various depths between measurement and simulation.

Fig. 5. Comparison of soil water potential between measurement and simulations with the inferred parameter values and recommended values by the FAO56 at 10 cm depth (a), 30 cm depth (b), 50 cm depth (c), 70 cm depth (d) and 90 cm depth (e).

Fig. 6. Inferred daily simulated coefficients for soil evaporation K_e and crop transpiration K_{cb} (a) and simple crop coefficient K_c (b).

Fig. 7. Cumulative potential and simulated evapotranspiration and rainfall plus irrigation in the experiment.

Fig. 8. Relationship between modeled rooting depth and cumulative day air temperature during growth.

Fig. 9. Effect of root shape parameter α_z on the overall comparison of soil water potential at depths between measurement and simulation. Symbols ◊, Δ, ×, * and ○ represents the simulations from a_z = 0.02, 0.025, 0.03, 0.035 and 0.04 cm^{-1}.

Table 1
Soil physical properties and the van Genuchten hydraulic parameter values

	Clay (%) (<0.002mm)	Silt (%) (0.002 - 0.05mm)	Sand (%) (> 0.05mm)	Organic matter (%)	Bulk density (g cm^{-3})	θ_s[a] (cm^3 cm^{-3})	θ_r[a] (cm^3 cm^{-3})	α[b] (cm^{-1})	n[b] (-)	K_s[c] (cm d^{-1})
Topsoil (0 – 30 cm)	13.0	11.5	75.5	1.7	1.55	0.374	0.025	0.07119	1.283	73.0
Subsoil (30 cm –)	11.0	10.0	79.0	0.8	1.65	0.342	0.025	0.06173	1.346	174.8

[a] θ_s, θ_r: the saturated and residual soil water contents, respectively;

[b] α, n: the shape parameters of the retention and conductivity functions, respectively;

[c] K_S: the saturated hydraulic conductivity.

Table 2
Dates and amounts (mm) of irrigations in different treatments

Treatment	05-May	06-May	12-May	02-Jun	24-Jun	25-Jun	29-Jun	30-Jun	07-Jul	19-Aug
1st	6.4	6.4	9.6	3.1	14.8	5.6	15.0	4.4	20.7	23.8
2nd	6.4	6.4	9.6	3.1	0.0	0.0	0.0	0.0	30.7	0.0
3rd	6.4	6.4	9.6	3.1	0.0	0.0	0.0	0.0	0.0	0.0

Table 3
Summary of the experiment

Soil type	Crop	Sowing date	Harvest date	Dry weight at harvest (t ha^{-1})	Max. rooting depth (cm)	Initial soil moisture (cm^3 cm^{-3})		
						0-30cm	30-60cm	60-90cm
Sandy loam	Dutch white cabbage	29 April 2009	8 September 2009	13.2	140.0	0.20	0.21	0.24

Table 4
Fitted coefficients of linear equation without the intercept and R^2 value between measurement and simulation of soil water potential at depths using different root shape parameter a_z

α_z (cm^{-1})	0.02	0.025	0.03	0.035	0.04
Gradient	1.419	1.342	1.183	0.896	0.56
R^2	0.532	0.668	0.716	0.498	0.009

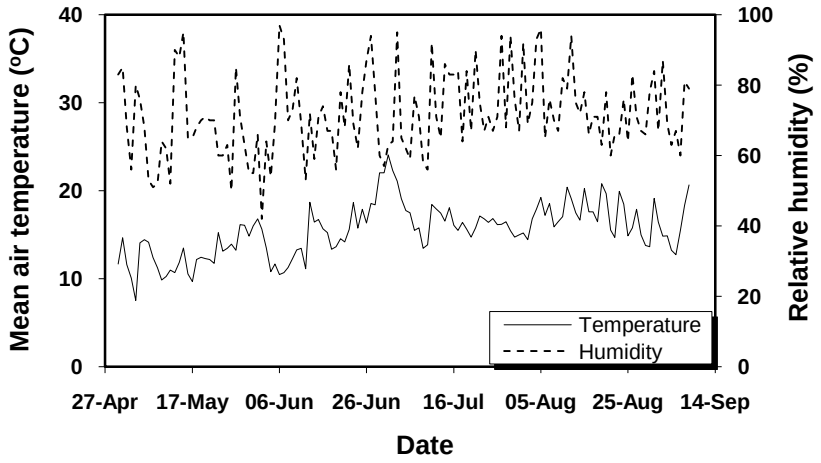
Mean air temperature (°C)
Relative humidity (%)
Temperature
Humidity
27-Apr
17-May
06-Jun
26-Jun
16-Jul
05-Aug
25-Aug
14-Sep
Date

(a)

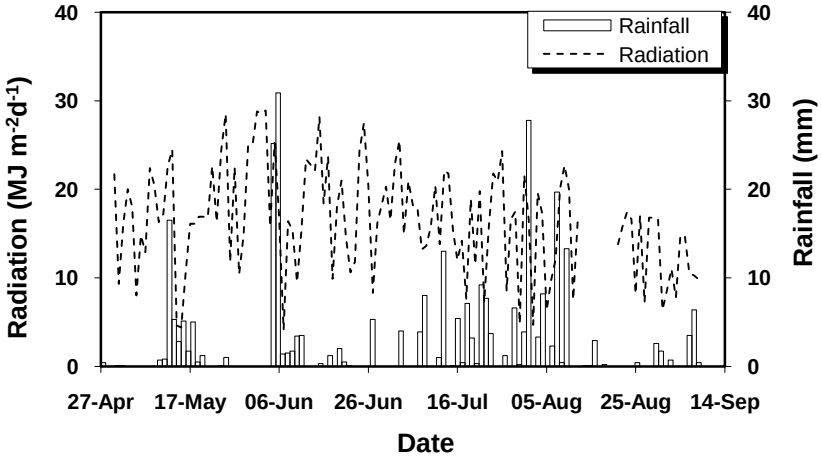
Radiation (MJ m-2d-1)
Rainfall (mm)
Rainfall
Radiation
27-Apr
17-May
06-Jun
26-Jun
16-Jul
05-Aug
25-Aug
14-Sep
Date

(b)

Fig. 1

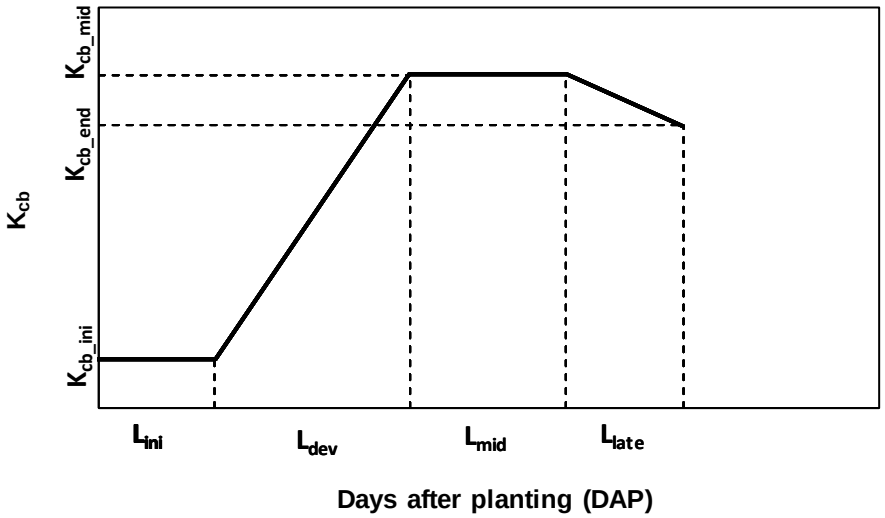
K_{cb}
K_{cb_mid}
K_{cb_end}
K_{cb_ini}
L_{ini}
L_{dev}
L_{mid}
L_{late}
Days after planting (DAP)

Fig. 2

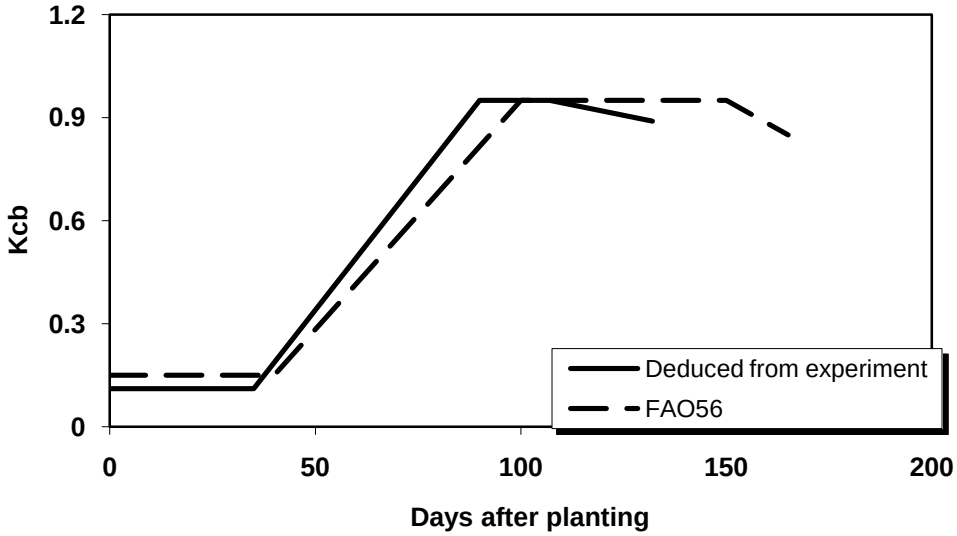
1.2
0.9
0.6
0.3
0
Kcb
0
50
100
150
200
Days after planting
Deduced from experiment
FAO56

Fig. 3

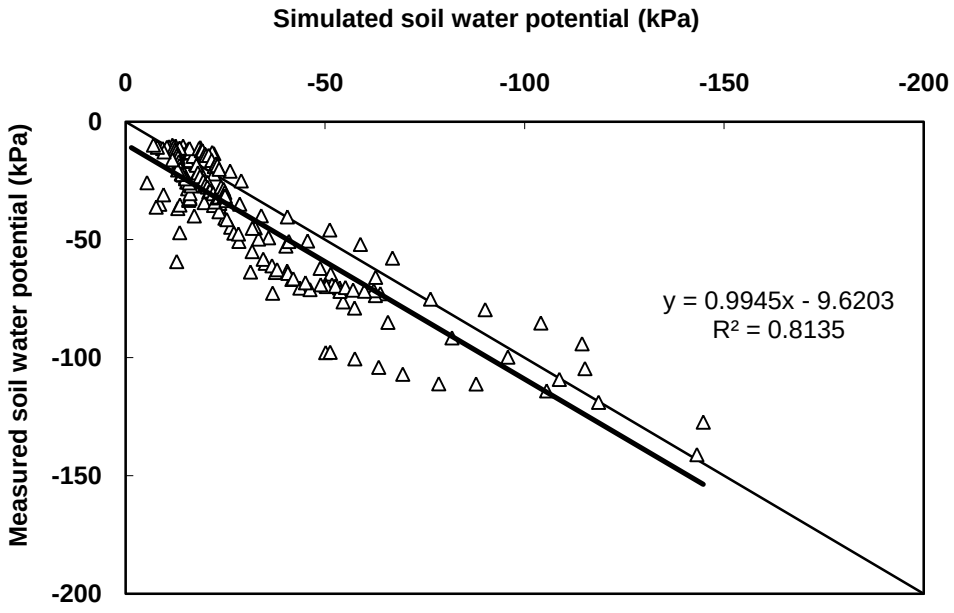
Simulated soil water potential (kPa)
0
-50
-100
-150
-200
Measured soil water potential (kPa)
0
-50
-100
-150
-200
y = 0.9945x - 9.6203
R² = 0.8135

Fig. 4

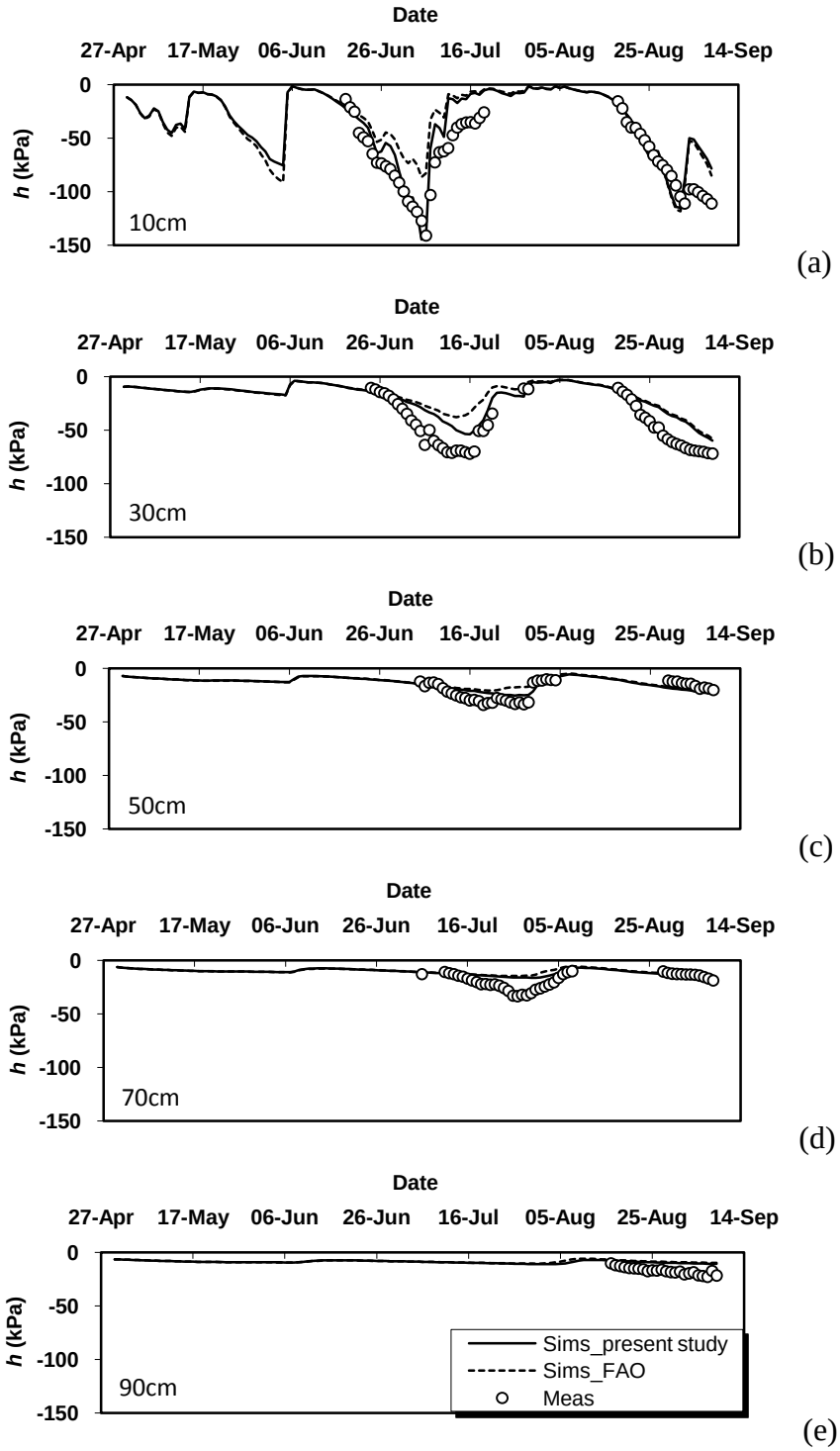
Date
27-Apr
17-May
06-Jun
26-Jun
16-Jul
05-Aug
25-Aug
14-Sep
h (kPa)
0
-50
-100
-150
10cm
(a)
30cm
(b)
50cm
(c)
70cm
(d)
90cm
Sims_present study
Sims_FAO
Meas
(e)

Fig. 5

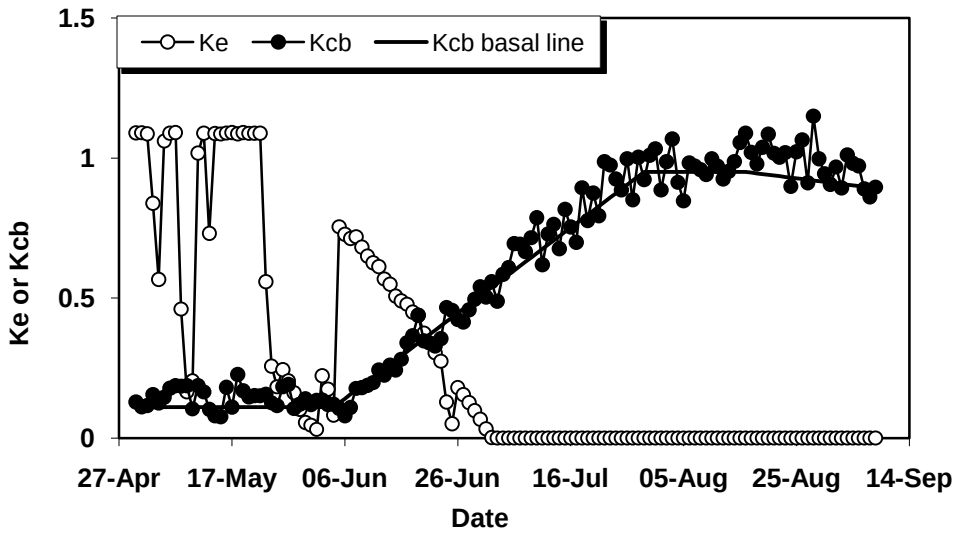
Ke
Kcb
Kcb basal line
Ke or Kcb
1.5
1
0.5
0
27-Apr
17-May
06-Jun
26-Jun
16-Jul
05-Aug
25-Aug
14-Sep
Date

(a)

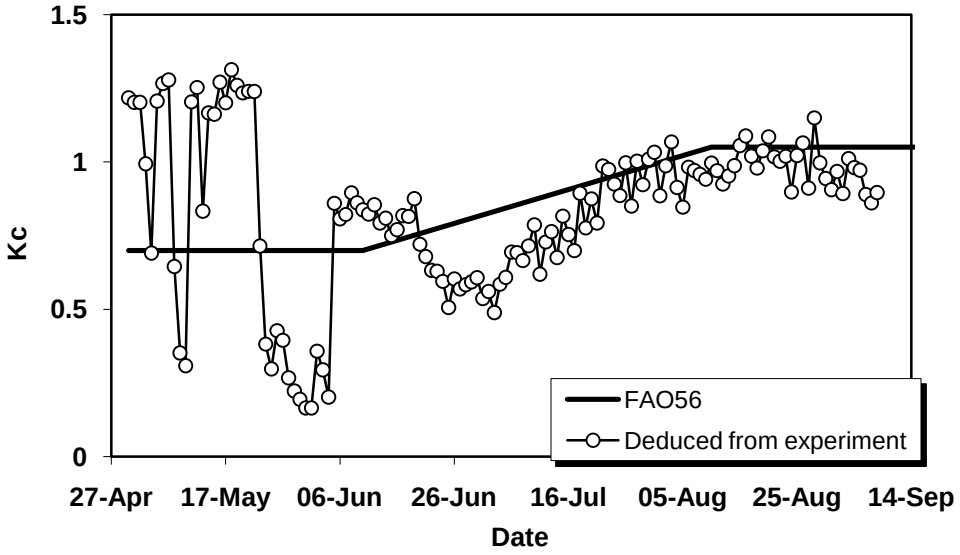
Kc
1.5
1
0.5
0
FAO56
Deduced from experiment
27-Apr
17-May
06-Jun
26-Jun
16-Jul
05-Aug
25-Aug
14-Sep
Date

(b)

Fig. 6

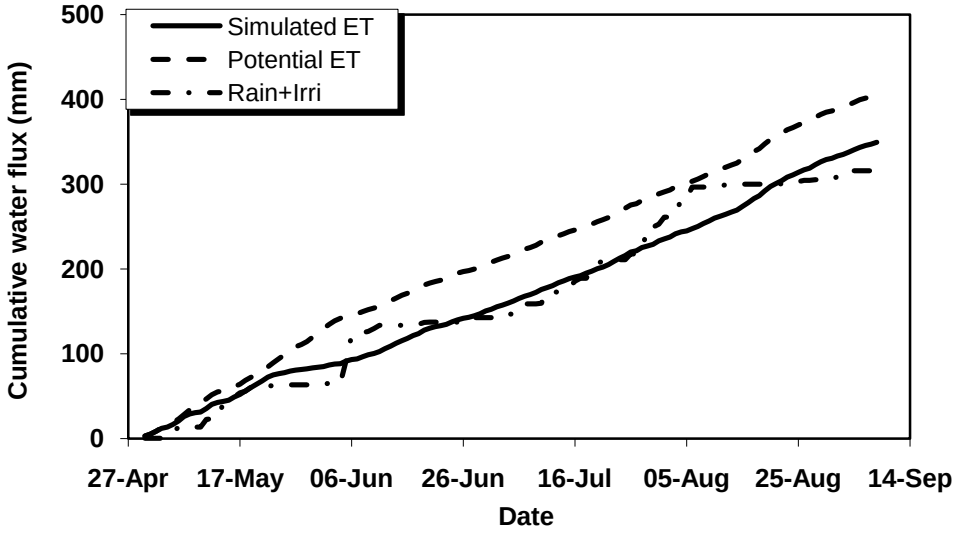
Simulated ET
Potential ET
Rain+Irri
Cumulative water flux (mm)
500
400
300
200
100
0
27-Apr
17-May
06-Jun
26-Jun
16-Jul
05-Aug
25-Aug
14-Sep
Date

Fig. 7

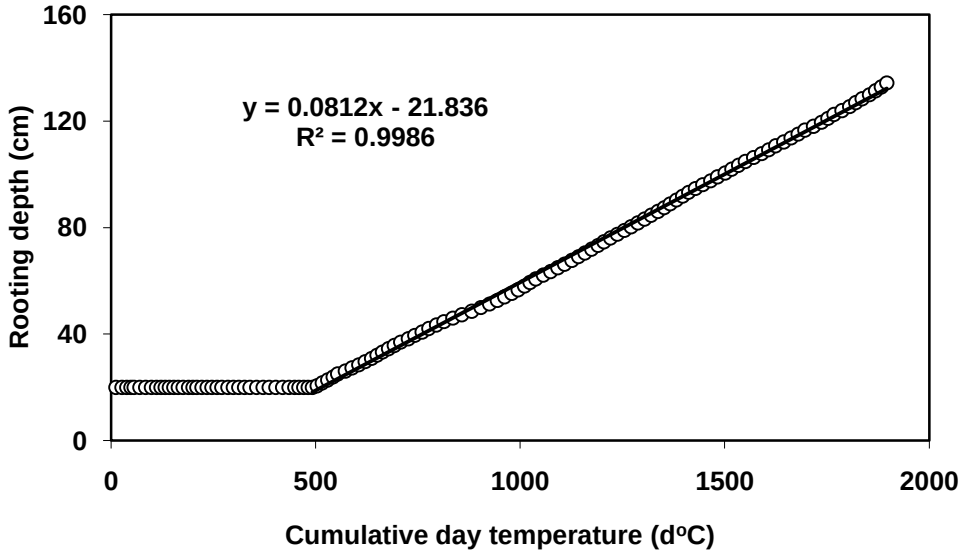
y = 0.0812x - 21.836
R² = 0.9986
Rooting depth (cm)
160
120
80
40
0
0
500
1000
1500
2000
Cumulative day temperature (dºC)

Fig. 8

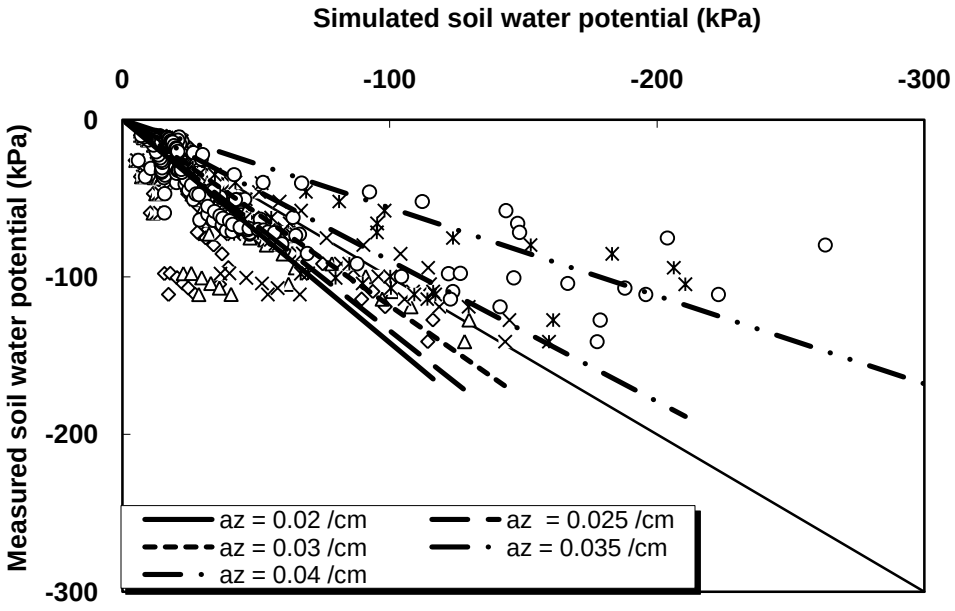
Simulated soil water potential (kPa)
0
-100
-200
-300
Measured soil water potential (kPa)
0
-100
-200
-300
az = 0.02 /cm
az = 0.025 /cm
az = 0.03 /cm
az = 0.035 /cm
az = 0.04 /cm

Fig. 9